

## Characterization of $\text{Co}_{1-x}\text{Zn}_x\text{Fe}_2\text{O}_4$ Nano Spinal Ferrites Prepared By Citrate Precursor Method

Ch. Vinuthna<sup>1</sup>, D. Ravinder<sup>2</sup>, R. Madhusudan Raju<sup>3</sup>.

<sup>1</sup>. Department of Chemistry, Osmania University, Hyderabad-500007, A.P. India.

<sup>2</sup>. Department of Physics, Nizam College, Bashbeerbagh, Osmania University, Hyderabad- 500001, Andhra Pradesh, India.

<sup>3</sup>. Department of Chemistry, College of Technology, Osmania University, Hyderabad- 500007, A.P. India.

### ABSTRACT

Cobalt-zinc ferrite nano-particles  $\text{Co}_{1-x}\text{Zn}_x\text{Fe}_2\text{O}_4$  were prepared by citrate precursor method, using cobalt, zinc, iron nitrates and citric acid as the organic precursor. Structural and morphological properties of the Ferrites were determined and characterized in detail by X-ray powder diffractometry (XRD), X-ray photo electron spectroscopy (XPS), Thermogravimetric analysis (TGA) and Infrared (IR) spectroscopy. X-ray diffraction pattern confirm the existence of single phase of cubic spinel crystal structure and the mean particle size of the nano-powders was calculated by Scherrer formula. Crystalline nature of the powder was observed when it was calcined at 500 °C. This study presents the effects of substitution of  $\text{Zn}^{2+}$  on the structural properties of cobalt-zinc ferrite nano-particles. The observed variation in Crystalline size and increase in lattice constant are endorsed due to the  $\text{Zn}^{2+}$  substitution in ferrites is reported. The unit cell parameter is found to increase linearly with increasing concentration of zinc due to larger ionic radii of  $\text{Zn}^{2+}$  ion. Fourier transformed infrared (FT-IR) spectra of  $\text{Zn}^{2+}$  ions substituted in Co-Zn spinal ferrite nano-particles have been analyzed in frequency range of 4000-400  $\text{cm}^{-1}$ . Two absorption bands in IR spectra were observed in the frequency range of 600-400  $\text{cm}^{-1}$  may be caused by the metal-oxygen vibrations in octahedral and tetrahedral sites.

Key words: Nano-particles, Ferrites, Cobalt-zinc, XPS, XRD.

### I. INTRODUCTION

Cobalt-zinc ferrite nano-particles exhibit exclusive chemical and physical properties [1-2]. Studies of spinel ferrites are highly relevant to current technologies such as magnetic cell separation, switching devices, permanent magnets, flexible recording media, hard disc recording media, detoxification of biological fluids, magnetically controlled transport of anti-cancer drugs and recording tapes, hence the synthesis and sintering of ferrites have become a vital part of modern technology [3-8]. Different techniques have been suggested for the preparation of nano ferrite materials but in present study citrate precursor method has been used for the preparation of cobalt-zinc ferrite materials, which is most convenient and yields more homogenous nano materials at lower processing temperatures. Thus, it presents a large superficial area and good sinterability in relation to powders obtained by other synthesis techniques.

Spinel ferrite nano-particles have engrossed much attention because of their electronic, magnetic, and catalytic properties. Spinel ferrites have the focus of intense in research for more than a decade due to their exclusive crystallographic structure and microstructure. Cations distribution of cobalt-zinc ferrites can be represented by  $\text{Zn}^{2+}_x\text{Fe}^{3+}_{1-x}[\text{Co}^{2+}_{1-x}\text{Fe}^{3+}_{1+x}]\text{O}_4$ . The Cation  $\text{Co}^{2+}$  in the cobalt-zinc ferrite promotes the exchange reaction  $\text{Co}^{2+} + \text{Fe}^{3+} \rightleftharpoons \text{Co}^{3+} +$

$\text{Fe}^{2+}$  in octahedral sites, whereas tetrahedral sites are preferentially occupied by zinc cations. In the above reaction  $\text{Co}^{2+}$  is reducing agent which reduces  $\text{Fe}^{3+}$  to  $\text{Fe}^{2+}$  ion, therefore the Cobaltous ion (Cobalt II ion) is changed to Cobaltic ion (Cobalt III ion) where as Ferric ion (iron III ion) is converted to Ferrous ion (iron II ion). This electron exchange reaction results the electronic conduction mechanism in cobalt-zinc ferrites.  $\text{CoFe}_2\text{O}_4$  has inverse spinel structure with  $\text{Co}^{2+}$  ions in octahedral sites and  $\text{Fe}^{3+}$  ions equally distributed between tetrahedral and octahedral sites whereas pure  $\text{ZnFe}_2\text{O}_4$  has a normal spinel structure with  $\text{Zn}^{2+}$  ions in tetrahedral and  $\text{Fe}^{3+}$  in octahedral sites, Zn-substitution in  $\text{CoFe}_2\text{O}_4$  results mixed cobalt-zinc ferrites which may endure Jahn-Teller distortion. The Zinc substitution affects the lattice parameter in ferrites as the Zinc is incorporated in to the cobalt ferrite the lattice constant is observed to increase representing Zinc substitution occurred. The crystal structure of a material can be described in terms of its unit cell. The unit cell is a containing one or more atoms arranged in 3-dimension and is given by its lattice parameters, which are the length of the cell edges and the angles between them, while the positions of the atoms inside the unit cell are described by the set of atomic positions measured from a lattice point. Lattice constant is affected by the surface reconstruction that results in a deviation from its mean value. This deviation is especially important in ferrite

nano-crystals since surface to nano-crystal core ratio is large [9]

## II. EXPERIMENTAL

### Preparation of $\text{Co}_{1-x}\text{Zn}_x\text{Fe}_2\text{O}_4$ spinel ferrite nanoparticles

The mixed  $\text{Co}_{1-x}\text{Zn}_x\text{Fe}_2\text{O}_4$  ferrite nanoparticles were synthesized by Citrate Precursor Method using Raw Materials Cobalt nitrate, Zinc nitrate, and Citric acid and Iron nitrate. All raw materials were mixed with deionized water individually, thus solution formed is mixed together except iron nitrate and  $\text{pH}$  is maintained at 7 by addition of ammonia followed by the addition of iron nitrate solution drop by drop with continuous stirring. The resulting solution was turned into gel when heated at  $80^\circ\text{C}$  on a hot plate. Then on combustion, burnt ash was formed which was calcined at  $500^\circ\text{C}$  for 4 hours.

### Powder X-ray Diffraction (XRD) analysis

Powder X-ray diffraction (XRD) patterns of all nano materials were obtained using a Ultima-IV diffractometer (M/s. Rigaku Corporation, Japan) operated at 40 kV and 20mA, using nickel filtered  $\text{Cu K}\alpha$  radiation ( $\lambda=1.54178 \text{ \AA}$ ). The samples were recorded in the  $2\theta$  range of  $10^\circ$ -  $80^\circ$  with a scan speed of  $2^\circ \text{ min}^{-1}$ .

### XPS analysis

X-ray Photoelectron Spectroscopy (XPS) is one of the most accepted and useful technique for study the composition of the samples. KRATOS AXIS165 X-ray photoelectron spectrometer (UK) with  $\text{Mg K}\alpha$  monochromatic excited radiation (1253.6 eV) was used for the analysis. The binding energy (BE) measurements were corrected for charging effects with reference to the C 1s peak of the adventitious carbon (284.6 eV).The X-ray gun was operated at voltage of 15 kV and current of 20mA. The analyzer chamber was degasified and pressure kept at  $1.33 \times 10^{-6}$  Pa. Survey and high resolution spectra were collected using 80 and 40 eV pass energy.

### FT-IR analysis

Fourier transform infrared (FT-IR) spectroscopy technique provides useful information about the nature and structure of ferrites. Infrared spectroscopy deals with the interaction of infrared radiation with matter. Fourier transform are a mathematical operation used to translate a complex curve into its component curves. FTIR relies on the fact that the most molecules of sample absorb light in the infrared region of the electromagnetic spectrum. These absorption peaks corresponds specifically to the bonds present in the molecule. The sample is irradiated by a broad spectrum of infrared light and the level of absorbance at a particular frequency is plotted after Fourier transforming the data. The resulting spectrum is characteristic of the bonds present in the sample.

FTIR spectra were obtained using a Thermo Nicolet Nexus 670 spectrometer. Minimum of 32 scans was signal-averaged with a resolution of  $2 \text{ cm}^{-1}$  within the wavelength range of  $400\text{-}4000 \text{ cm}^{-1}$ . Small and diluted drop of the nanoferrite samples were prepared and coated on KBr disks and stored at room temperature. In order to remove the residual solvent, KBr disks were dried at  $80^\circ\text{C}$  under vacuum.

### Thermo-gravimetric (TG) analysis

Thermogravimetric experiments were performed using a TGA/DTA 851° THERMAL SYSTEM (mettler Toledo, Switzerland) at a heating rate of  $10^\circ\text{C min}^{-1}$  in the temperature range of  $25\text{-}800^\circ\text{C}$  under  $\text{N}_2$  atmosphere (flow rate  $30 \text{ mL min}^{-1}$ ). The powder samples ranging from 8-10 mg weighed and heated on a pan. During this process temperature difference and weight loss were recorded as a function of temperature.

## III. RESULTS AND DISCUSSION

### 3.1 X-ray diffraction (XRD)

Fig.1 shows the XRD patterns for all the samples of Cobalt-Zinc ferrites nano-particles. The figure shows cubic spinel structure. The diffraction peaks are broad because of the nanometer size of the crystallite.

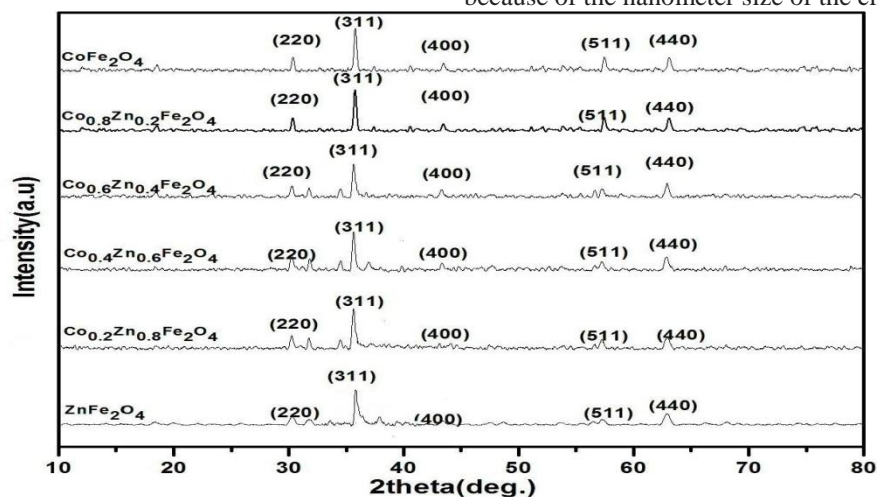


Fig.1 XRD pattern of the Cobalt-Zinc nano--ferrites

The powdered samples were characterized by XRD for structural determination and particle size calculation. The indexed XRD patterns of the Cobalt-Zinc-ferrites calcinated at 500°C are shown in Fig.1. The particle sizes for all samples prepared have been calculated from the Debye-Scherrer's equation. While taking the instrumental broadening into account.

$$D_{hkl} = \frac{0.91\lambda}{\beta \cos\theta}$$

Where D is the crystallite size, λ is the wavelength of X-ray radiation [10]used, θ is the Bragg angle and β is the full width at half maximum (FWHM) of the most intense diffraction peak. The crystallite size is in the range of 21-28nm for the different compositions, shown in table I. all the peaks are characteristics for the cubic structure and spinal type lattice of cobalt-Zinc ferrites. The sharpness of the peaks decides the crystallinity of the samples.

**Table 1: Values of Crystallite size, Lattice parameter (a) and hopping length for A-site (d<sub>A</sub>) and B-site (d<sub>B</sub>) of Co-Zn ferrite nano-particles**

SAMPLE	Crystallite size (nm)	Lattice Parameter(a) A°	Vol of Unit Cell(V) (A°) <sup>3</sup>	A site (d <sub>A</sub> )	B site (d <sub>B</sub> )
CoFe <sub>2</sub> O <sub>4</sub>	28.00	8.37	586	2.959	3.624
Co <sub>0.8</sub> Zn <sub>0.2</sub> Fe <sub>2</sub> O <sub>4</sub>	26.89	8.36	584	2.955	3.619
Co <sub>0.6</sub> Zn <sub>0.4</sub> Fe <sub>2</sub> O <sub>4</sub>	26.38	8.39	590	2.967	3.633
Co <sub>0.4</sub> Zn <sub>0.6</sub> Fe <sub>2</sub> O <sub>4</sub>	24.08	8.40	592	2.972	3.640
Co <sub>0.2</sub> Zn <sub>0.8</sub> Fe <sub>2</sub> O <sub>4</sub>	22.44	8.43	599	2.982	3.652
ZnFe <sub>2</sub> O <sub>4</sub>	21.50	8.49	611	2.982	3.653

The lattice parameter of samples was established from X-ray studies by using the following equation. Which are shown in table.1

$$a = d \sqrt{h^2 + k^2 + l^2} \text{ [A}^0\text{]}$$

Where (h k l) --- are the Miller Indices, d --- Is inter planner spacing.

Thus lattice parameter was computed using the d value and the (hkl) parameters, all samples obeys Vegard's law [11]. Lattice parameter increases with increasing the zinc substitution giving the evidence that Zn is substituted in cobalt ferrite.

The Volume of the Unit Cell is calculated by using the following equation, which depends on the Lattice Parameter. The Unit cell values increases with increasing the zinc substitution in cobalt ferrite. Values are shown in Table I.

$$\text{Volume of the Unit Cell } V = a^3 \text{ [A}^0\text{]}^3$$

The distance between magnetic ions on B and A Sites is calculated according to the following relations [12]

$$d_A = 0.25 a\sqrt{2} \quad \text{and} \quad d_B = 0.25 a\sqrt{3}$$

Where (a) ---is the lattice parameter  
 The values of the hopping length for octahedral (d<sub>A</sub>) and tetrahedral (d<sub>B</sub>) sites are listed in Table I. It is clear that the distance between the magnetic ions increases as the Zn content increases.

### 3.2. X-ray Photoelectron Spectroscopy (XPS)

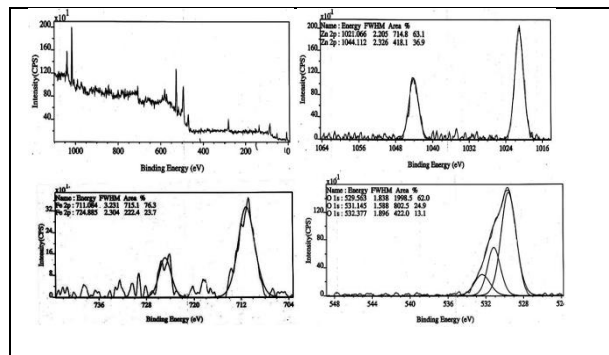


**Fig.2 XPS patterns of ZnFe<sub>2</sub>O<sub>4</sub>**

X-ray photo electron spectroscopy (XPS) gives information about the oxidation state and chemical stoichio-metric composition in the samples. In this procedure emission of electrons takes place from atoms and resides near the surface of the material without losing energy, and so surface sensitive features are achievable. Chemical depth summary information can be obtained by variation of the angle of incident of radiation. The low resolution XPS has the capability to determine the elemental composition on the surface of all nonvolatile materials.

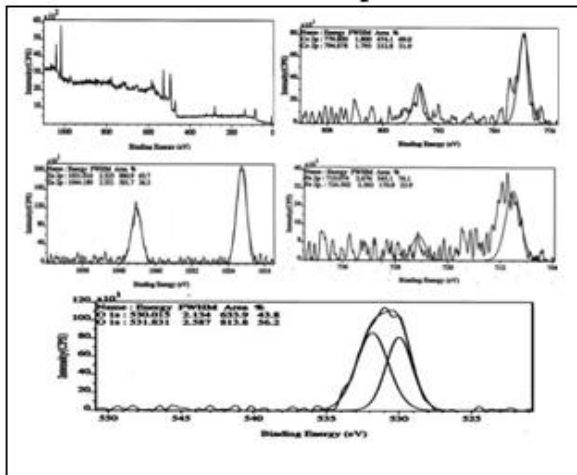


Fig.3. XPS of  $\text{Co}_{0.8}\text{Zn}_{0.2}\text{Fe}_2\text{O}_4$

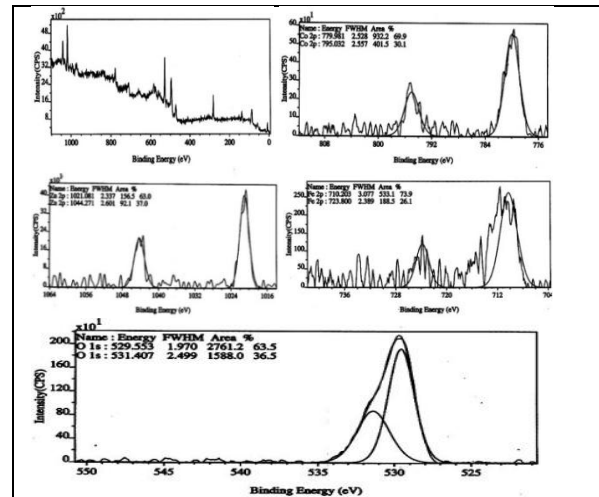


Fig.6 XPS of  $\text{Co}_{0.2}\text{Zn}_{0.8}\text{Fe}_2\text{O}_4$

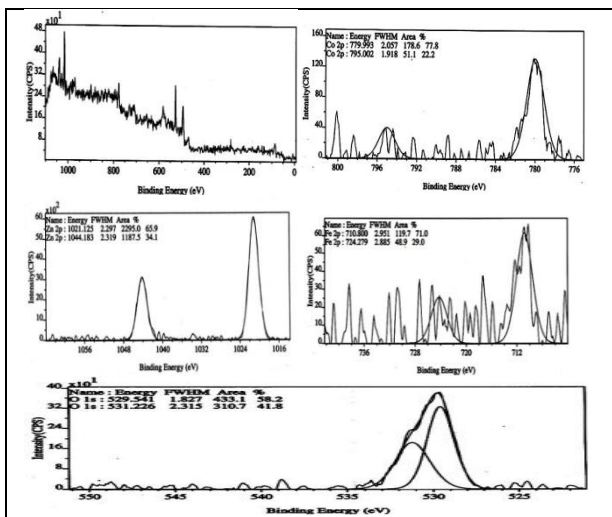


Fig.4. XPS of  $\text{Co}_{0.6}\text{Zn}_{0.4}\text{Fe}_2\text{O}_4$

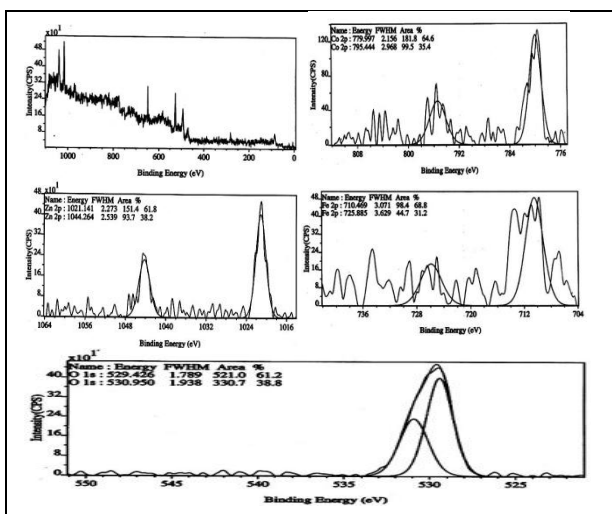


Fig.5 XPS of  $\text{Co}_{0.4}\text{Zn}_{0.6}\text{Fe}_2\text{O}_4$

The binding energies (BEs) of  $\text{Co}2p$ ,  $\text{Zn}2p$ ,  $\text{Fe}2p$ , and  $\text{O}1s$  are listed in Table 2. The BEs of  $\text{Co}2p$ ,  $\text{Zn}2p$ ,  $\text{Fe}2p$ , are ascribed to the BEs of  $\text{Co}^{2+}$ ,  $\text{Zn}^{2+}$ , and  $\text{Fe}^{3+}$  ionic states in the samples. The spinel crystalline structure ( $\text{AB}_2\text{O}_4$ ) with tetrahedral and octahedral site for metal atoms is conformed.

Zn exhibits binding energies at 1021 eV and 1044 eV, which corresponds to  $\text{Zn}2p_{3/2}$  and  $\text{Zn}2p_{1/2}$  electrons in the  $\text{Zn}^{2+}$  oxidation state (13) respectively. The FWHM values of  $\text{Zn}2p_{3/2}$  shown variation from 2.2eV to 2.5 eV, signifying that the chemical environment of Zn atom has changed from sample to sample in substitution process.

Generally,  $\text{Fe}2p$  states of the Fe atom could be used to distinguish the variation between  $\text{Fe}^{2+}$  and  $\text{Fe}^{3+}$ . The peaks of  $\text{Fe}2p_{3/2}$  and  $\text{Fe}2p_{1/2}$  states can be observed in the range of 710-711 eV, and 724-725 eV. The peak with the range of 710-711 eV is attributed to the  $\text{Fe}^{3+}$  Cation located at the octahedral site in the spinel structure. The peak range of 724,725 is endorsed to the  $\text{Fe}^{2+}$  Cation located at the tetrahedral site in the spinel structure.

The  $\text{Co}2p$  XPS spectra show two major peaks with binding energy values at 794,795 and 779 eV, corresponding to the  $\text{Co}2p_{1/2}$  and  $\text{Co}2p_{3/2}$  spin-orbit peaks, respectively, of the  $\text{CoO}$  phase. (14)

The  $\text{O}1s$  spectrum shows the existence of oxygen in two different states, with binding energies at 529,530 eV and 531,530 eV that can be assigning to the lattice-oxygen and the oxygen-deficient regions, respectively. The peak observed close to 531 eV in the  $\text{O}1s$  spectra indicate the presence of  $-\text{OH}$  (hydroxyl) species adsorbed on the surface to the samples due experimental conditions. The XPS measurement results were related to XRD observations conforming the single cubic phase of the ferrite.

3.3. FTIR

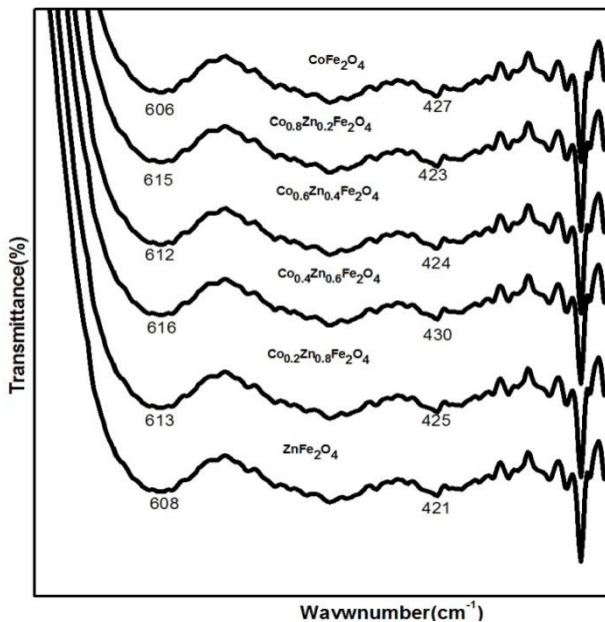


Fig.7 FT-IR spectra of Cobalt-Zinc-ferrites

The FT-IR spectra explain the position of the ions in the crystal structure and their vibration modes. The two common bands in almost all spinel ferrite are found in the region of 600cm<sup>-1</sup> and 400 cm<sup>-1</sup>. The frequency bands close to 606-616 cm<sup>-1</sup> and 421-430 cm<sup>-1</sup> are assigned to the tetrahedral and octahedral clusters and also confirm the presence of M-O stretching band in ferrites, thus the vibrational mode of tetrahedral clusters is higher as compared to that of octahedral clusters, which is responsible for the shorter bond length of tetrahedral clusters. (15)

3.4 TGA

The thermo-gravimetric(TG) study of Co<sub>0.4</sub>Zn<sub>0.6</sub>Fe<sub>2</sub>O<sub>4</sub> shows a graph in the range of 30 to 800°C .weight loss started from 100°C onwards which is gradually increased with slight difference ,and when reached to 800°C no such loss is observed suggests that the hydroxyl groups are not present in nanoferrite.

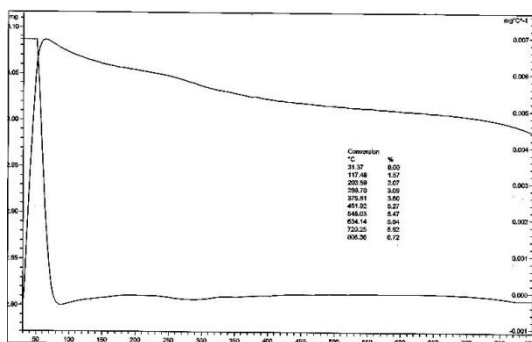


Fig.8 TGA of Co<sub>0.6</sub>Zn<sub>0.4</sub>Fe<sub>2</sub>O<sub>4</sub>

- Citrate precursor method used was very suitable and most excellent method because of improved micro-structural and composition control achievable.
- X- ray diffraction pattern confirm that the formation of cubic spinel structure in single phase without any impurity peak.
- The Crystallite size of the ferrite powder was in the range 21-28 nm.
- The lattice parameter, the distance between magnetic ions on B and A Sites is calculate which increases with increasing Zn substituted in Co ferrites is.
- XPS gives information about the oxidation state and chemical stoichiometric composition of the samples. The oxidation states of transitions metals were Co<sup>2+</sup>, Zn<sup>2+</sup>, and Fe<sup>3+</sup> in the samples.
- FT-IR spectra explain tetrahedral and octahedral clusters and also confirm the presence of M-O stretching band in ferrites.
- TGA analysis conforms that the moisture content decreases when the samples were calcinated

ACKNOWLEDGEMENTS

One of the authors D.R is grateful to Prof. T.L.N. Swamy, Principal Nizam College for his encouragement to carry out this research work. The authors are thankful to Prof. C. Gyana Kumari, Head, Department of Chemistry, Osmania University, and Hyderabad for her encouragement in carrying out the research activities.

REFERENCES

- [1] Ball, P., Li, G. (1992), Science at the atomic scale. *Nature*, 355,761-765.
- [2] Cavicchi, R.E., Silsbe, R.H, Coulomb Suppression of Tunneling Rate from Small Metal Particles, *Phys. Rev. Lett*, 52(16), 1984,1453-1456.
- [3] N. M. Deraz, S. Shaban, Optimization of catalytic, surface and magnetic properties of nanocrystalline manganese ferrite, *J. Analyt. Appl. Pyrolysis*, 86(1),2009,173-179.
- [4] N. M. Deraz, M. K. El- Aiashy, Suzan. A. Ali, Novel Preparation and Physicochemical Characterization of a Nanocrystalline Cobalt Ferrite System, *Adsorp. Sci. Technol*, 27(8),2009,797-803.
- [5] N.M. Deraz, S.A. Shaban, A. Alarifi, Removal of sulfur from commercial kerosene using nanocrystalline NiFe<sub>2</sub>O<sub>4</sub> based sorbents *J. Saudi Chemical Society*, 14(4),2010, 357-362.

IV. CONCLUSIONS

- [6] Y. KÖseoglu, A. Baykal, F. Gzüak, H. Kavas, Structural and magnetic properties of  $\text{Co}_x\text{Zn}_{1-x}\text{Fe}_2\text{O}_4$  nanocrystals synthesized by microwave method, *Polyhedron*, 28 (14), 2009, 2887-2892.
- [7] Shao-Wen Cao, Ying-Jie Zhu, Guo-Feng Cheng, Yue-Hong Huang,  $\text{ZnFe}_2\text{O}_4$  nanoparticles: Ionic liquid synthesis and photocatalytic property over phenol, *Journal of Hazard. Material*. 171 (1), 2009, 431-435.
- [8] Z.H. Zhou, J.M. Xue, J. Wang, H.S.O. Chan, T. Yu, Z.X. Shen,  $\text{NiFe}_2\text{O}_4$  nanoparticles formed in situ in silica matrix by mechanical activation, *Journal of Applied Physics*, 91(9), 2002, 6015-6020.
- [9] Mudar A. Abdulsattar, Ab initio large unit cell calculations of the electronic structure of diamond nanocrystals, *Solid State Sciences*, 13(5), 2011, 843-849.
- [10] B. D. Cullity, Elements of X-ray diffraction, Wesley Pub.Co.Boston., 101-356(1987).
- [11] L. Vergard, *Z. Phys.*, 5, 17(1921).
- [12] B.Viswanathan, V. R.K. Murthy Ferrite Materials Science and Technology NarosaPubl House, New Delhi (1990)
- [13] Munusamy vijayaraj, chinnakonda S.Gopinath, On the Active spacer and stabilizer role of Zn in  $\text{Cu}_{1-x}\text{Zn}_x\text{Fe}_2\text{O}_4$  in the selective mono-N-methylation of aniline: XPS and catalysis study, *journal of catalysis*, 241, 2006, 83-95.
- [14] Lijun Zhao, Hongjie Zhang, Yan Xing, Shuyan Song, Shiyong Yu, Weidong Shi, Xianmin Guo, Jianhui Yang, Yongqian Lei, Feng Cao, Studies on the magnetism of Cobalt ferrite nanocrystals synthesized by hydrothermal method, *J.Solid State.chem*, 181, 245-252.
- [15] P. Pramanik, A novel chemical route for the preparation of nanosized oxide, phosphorus, vanadates, molybdates & tungstates in polymer process, *bull. mater. SCI*, 22(3), 1999, 335-339.

**Table 2. Binding Energies of Cobalt-Zinc ferrites**

Sample name	Binding Energy (eV)							
	Co		Zn		Fe		O	
	2p <sub>3/2</sub>	2p <sub>1/2</sub>	2p <sub>3/2</sub>	2p <sub>1/2</sub>	2p <sub>3/2</sub>	2p <sub>1/2</sub>	1s	
ZnFe <sub>2</sub> O <sub>4</sub>		----	1021.06	1044.11	711.08	724.88	529.56	531.14
Co <sub>0.2</sub> Zn <sub>0.8</sub> Fe <sub>2</sub> O <sub>4</sub>	779.80	794.87	1021.12	1044.18	710.07	724.50	530.01	531.83
Co <sub>0.4</sub> Zn <sub>0.6</sub> Fe <sub>2</sub> O <sub>4</sub>	779.98	795.03	1021.01	1044.18	710.20	723.80	529.55	531.40
Co <sub>0.6</sub> Zn <sub>0.4</sub> Fe <sub>2</sub> O <sub>4</sub>	779.99	795.00	1021.14	1044.26	710.80	724.27	529.54	531.22
Co <sub>0.8</sub> Zn <sub>0.2</sub> Fe <sub>2</sub> O <sub>4</sub>	779.99	795.44	1021.08	1044.27	710.46	725.88	529.42	530.95